Selective water uptake within micelle-containing layer-by-layer films of various architectures: A neutron reflectometry study

ARTICLE *in* SOFT MATTER · OCTOBER 2012

Impact Factor: 4.03 · DOI: 10.1039/c2sm26583d

4 AUTHORS, INCLUDING:

Aliaksandr Zhuk
Johnson & Johnson, Skillman, US
10 PUBLICATIONS **175** CITATIONS
SEE PROFILE

John F Ankner
Oak Ridge National Laboratory
148 PUBLICATIONS **1,869** CITATIONS
SEE PROFILE

Svetlana Sukhishvili
Stevens Institute of Technology
134 PUBLICATIONS **4,811** CITATIONS
SEE PROFILE

Soft Matter

RSC Publishing

PAPER

View Article Online
View Journal | View Issue

Cite this: *Soft Matter*, 2013, 9, 410

Selective water uptake within micelle-containing layer-by-layer films of various architectures: a neutron reflectometry study†

Aliaksandr Zhuk,[a] Li Xu,[a] John F. Ankner*[b] and Svetlana A. Sukhishvili*[a]

Swelling of micelle-containing layer-by-layer (LbL) films of various architectures has been studied by neutron reflectometry (NR). Multilayers of the first type were constructed using poly(2-(dimethylamino) ethyl methacrylate)-*block*-poly(*N*-isopropylacrylamide) (PNIPAM-*b*-PDMA) block copolymer micelles (BCMs) alternately assembled with poly(4-styrene sulfonate) (PSS). NR data showed that the films maintained their layered structure, but deuterated PSS (*d*PSS), deposited within every 5th layer as a marker, was highly interdiffused into neighboring layers. *In situ* NR measurements demonstrated that the films swelled homogeneously by ~35% in an aqueous environment. The second type of multilayer contained three zones: bottom and top stacks consisting of PDMA/*d*PSS homopolymer assemblies, and BCMs deposited in the middle stack as (BCM/*d*PSS)$_n$, where n is the number of deposition cycles, equal to 1 or 2. The individual micellar layer deposited in a single deposition step ($n = 1$) only partially covered the surface, whereas a complete layer of micelles was achieved after two deposition cycles. *In situ* NR study of these stacked films revealed different degrees of water uptake by film internal strata. While layers of assembled micelles took up ~38% water by volume when dry films were exposed to an aqueous environment at 25 °C, the bottom homopolymer stack was able to take up only 11–20% water. In addition, the film architecture and the degree of surface coverage by BCMs were found to be important factors enabling the study of selective swelling of film strata. NR-enabled observations of selective swelling of assembled amphiphilic BCMs allow one to correlate film swelling on the nanoscale with internal structure, and present a powerful approach for future studies of BCM-containing systems, which are useful in actuation, sensing, and controlled delivery applications.

Received 8th July 2012
Accepted 3rd October 2012

DOI: 10.1039/c2sm26583d

www.rsc.org/softmatter

Introduction

Among the various types of functional soft materials, layer-by-layer (LbL) grown films are of great interest since this technique allows construction of nanoscopically structured films.[1] Multilayers are not thermodynamically stable structures, and film stratification depends on the binding energy of polymer pairs, which in turn defines the degree of layer interdiffusion.[2–5] Indeed, while originally thought of as films with relatively well-defined structures, multilayer films with high degrees of chain interpenetration or even with completely intermixed polymer coils can be produced.[2] The degree of chain interpenetration within LbL films is strongly dependent on the type of polyelectrolytes used in film deposition, and in the case of weak polyelectrolytes it is strongly influenced by solution pH[6–8] and ionic strength used during film deposition, or applied post-assembly. For example, addition of salt during deposition screens electrostatic interactions and enhances polymer interdiffusion within LbL films.[9–11] At the same time, post-assembly annealing of electrostatically assembled LbL films in high-ionic-strength solutions also induces layer intermixing.[12] Morphological changes within weak polyelectrolyte LbL films composed of poly(acrylic acid) and poly(allylamine) can also be triggered by immersing assembled films in an acidic solution.[13] Additionally, the internal structure of LbL films can also be regulated, to a lesser extent, by polymer concentration, molecular weight, deposition time and other factors.[14–16]

Neutron reflectometry (NR) and X-ray reflectivity (XR) are two uniquely suitable techniques for investigating the internal structure of LbL films on the nanoscale.[1,17,18] However, X-ray reflectometry requires sufficient electron density contrast and is useful only for studies of LbL films containing inorganic or/and metal nanoparticles. On the other hand, the use of deuterated polymers as markers within LbL films provides neutron scattering contrast and enables studies of the interior structure of all-organic LbL assemblies. Neutron reflectometry has been

[a]*Department of Chemistry, Chemical Biology and Biochemical Engineering, Stevens Institute of Technology, Castle Point on Hudson, Hoboken, NJ 07030, USA. E-mail: ssukhish@stevens.edu*

[b]*Spallation Neutron Source, Oak Ridge National Laboratory, Oak Ridge, TN 37831, USA*

† Electronic supplementary information (ESI) available. See DOI: 10.1039/c2sm26583d

applied to study the internal structure of both electrostatic and hydrogen-bonded LbL films.[19–21] However, to the best of our knowledge, all previous neutron reflectivity studies have focused on multilayer films obtained by assembly of homopolymers.

Among the different components used as building blocks in LbL assemblies, block copolymer micelles (BCMs) stand out as attractive candidates because of their ability to endow films with 'pockets' (*i.e.* micellar cores) which are not involved in intermolecular binding and are therefore available for trapping and controlled release of functional molecules. For example, the availability of such pockets within a film enhances the film loading capacity for drugs which have low solubility in water but can be accumulated in hydrophobic micellar cores. When micellar cores are composed of amphiphilic pH- or temperature-responsive polymers, they can 'open up' or 'close' on demand by the application of external stimuli, providing a means of controlling film swelling and loading or release of cargo molecules.

LbL assembly using BCMs as building blocks was studied for two different types of micelles, having either glassy cores or cores responsive to environmental stimuli. A distinct feature of responsive BCMs is that their core-forming blocks exhibit solubility–collapse transitions triggered by external stimuli. Monolayers of stimuli-responsive micelles adsorbed onto a solid substrate were first studied by Webber *et al.*[22] In that work, reversible pH-controlled uptake of water and dissolution of poly(2-(diethylamino)ethyl methacrylate) (PDEA) cores in adsorbed BCM monolayers was demonstrated. Multilayers of BCMs can also be constructed using reactive assembly,[23] electrostatically driven deposition of BCMs with a linear polymer,[24,25] or hydrogen-bonded assembly of micelles with protonated acid or polyphenol.[26–28] In addition, all-BCM multilayer films of two types of BCMs with cationic and anionic coronae have been deposited on both planar[29] and colloidal substrates.[30]

Immersing multilayers containing amphiphilic-core BCMs in water at a temperature below the lower critical solution temperature (LCST) of the micellar-forming block can trigger significant film swelling, resulting from uptake of water into the micellar cores. The amplitude of film swelling is determined by the nature and strength of the interactions between BCM coronae and their homopolymer counterparts, the ratio of core to corona block sizes of the copolymers, and deposition conditions. Zhu and Sukhishvili[28] and Xu *et al.*[31] reported on multilayers of diblock copolymer micelles with PNIPAM cores. When exposed to ambient temperatures below PNIPAM's LCST, these films took up 65% water by weight. Importantly, in spite of the dissolution of micellar cores at low temperatures, the micelles remained bound within the film through their corona chains and preserved their morphology. Recently, Tan *et al.* explored the swelling of LbL films composed of micelles of triblock copolymers with a poly(propylene oxide) (PPO) central block and poly(ethylene oxide) (PEO) corona, and polyanions, such as poly(4-styrene sulfonate) (PSS) or poly(acrylic acid) (PAA).[32] When PAA was used for BCM multilayer construction, water uptake increased from ~50% to 400% when the temperature was lowered through PPO's LCST. Interestingly, the use of PSS in place of PAA dramatically suppressed film swelling both below and above PPO's LCST as a result of strong ionic binding between the sulfonate groups of PSS and micellar corona chains. Swelling of micelle-containing LbL films of triblock and diblock copolymers of different molecular weights but the same corona-to-core block ratio was similar in amplitude while differing only in kinetics.[33] It has been shown that multilayers of triblock copolymers have higher stability to repeatedly applied external stimuli.[33]

In spite of the significant information resulting from studies of the overall film swelling using *in situ* ellipsometry and AFM techniques, the molecular mechanisms of film swelling, direct measurements of water uptake within the cores of assembled BCMs, as well as the quantitative relationship between the degree of water uptake within micellar cores and the overall film swelling have remained unexplored. Here, we take advantage of the ability of NR to resolve the internal structure of all-organic films and apply this technique to investigate the internal structure of BCM-containing LbL films at the nanoscale level, to assess the degree of interpenetration of the homopolymer and BCM layers within the films, and to quantify water uptake by specific strata. These studies open ways to study and rationally construct selectively swelling stratified films for a broad range of applications, including microfluidics, biomedicine and sensing.

Experimental methods

Materials

The PDMA-*b*-PNIPAM block copolymer was synthesized by atom transfer radical polymerization (ATRP) using ethyl 2-bromoisobutyrate as an initiator and copper(I) bromide/1,1,4,7,10,10-hexamethyltriethylene-tetramine as a catalyst–ligand pair. The synthetic procedure for the PDMA–Br macroinitiator and its use for preparation of PDMA-*b*-PNIPAM have been described elsewhere.[34,35] The weight-average molecular weights of PDMA and PNIPAM blocks were 8.6 and 4.7 kDa, respectively, as determined by a combination of gel permeation chromatography (GPC) and ^{1}H NMR. GPC studies of single PDMA block and block copolymers performed in tetrahydrofuran revealed polydispersity indexes of 1.10 and 1.25 for the PDMA block and the PDMA-*b*-PNIPAM copolymer, respectively. The block copolymer is abbreviated as $PDMA_{50}$-*b*-$PNIPAM_{25}$, where the subscript denotes the average number of monomer units in each copolymer block.

PDMA was synthesized by ATRP, as described elsewhere.[34] In brief, DMA (8.0 mL, 47 mmol), CuBr (33 mg, 0.23 mmol), 1,1,4,7,10,10-hexamethyltriethylenetetramine (HMTETA) (62 μL, 0.92 mmol) and 2-propanol (8.0 mL) were mixed into a 50 mL Schlenk flask. The solution was processed by three freeze–pump–thaw cycles, and then ethyl-2-bromoisobutyrate (34 μL, 0.23 mmol) was injected into the reaction solution under argon flow. After continuous stirring under the argon for 12 h the polymerization was terminated with liquid nitrogen and the solution was diluted with tetrahydrofuran (THF). Then the solution was passed through a basic aluminum oxide column to remove the catalyst

complex. After evaporation of the THF solvent, the obtained polymers were precipitated by cold hexane and dried in a vacuum oven at 30 °C overnight. The M_w of PDMA was determined to be ~30 kDa (PDI of 1.10) as measured by a combination of GPC and ^{1}H NMR.

Ultrapure Milli-Q water (Millipore) with a resistivity of 18 MΩ cm^{-1} was used in all experiments. Poly(4-styrene sulfonate), sodium salt (PSS, $M_w = 77$ kDa) and branched polyethylenimine (BPEI, $M_w = 25$ kDa) were purchased from Aldrich. Deuterated poly(4-styrene sulfonate) sodium salt (*d*PSS, $M_w = 55.8$ kDa) was purchased from Polymer Source, Inc. One-side-polished silicon wafers of 2″ diameter with (100) orientation and a resistivity of 0.001–0.005 Ω cm were purchased from the Institute of Electronic Materials Technology (Poland). All other chemicals were purchased from Aldrich and used without further purification.

Multilayer deposition

Prior to film deposition, wafers were cleaned using UV radiation for 2 hours then immersed in concentrated H_2SO_4 for 15 min, rinsed with Milli-Q water, immersed in a 0.1 M NaOH solution for 5 min, and finally thoroughly rinsed with Milli-Q water. Silicon wafers were primed with a BPEI precursor layer deposited by immersing the cleaned silicon substrates in a 0.2 mg mL^{-1} BPEI aqueous solution adjusted to pH 5.5 at 25 °C for 15 min, followed by rinsing with Milli-Q water and drying in a stream of nitrogen. The PDMA-*b*-PNIPAM block copolymer and polyelectrolytes were dissolved in a 0.01 M phosphate buffer solution which was then adjusted to a pH of 6.0. The formation of copolymer micelles was accomplished by heating the solution to 45 °C for 2 h. Multilayer systems of two types were constructed: (1) a BCM/PSS system of 19-bilayers consisting of a sequence BPEI/PSS/$[(\text{BCM/PSS})_4/(\text{BCM}/d\text{PSS})]_4/(\text{BCM/PSS})_4$ was deposited by sequential deposition of PDMA-*b*-PNIPAM micelles and PSS, where *d*PSS was deposited in every fifth bilayer to provide neutron scattering contrast, and (2) a stacked system with a sequence of BPEI/*d*PSS/$[(\text{PDMA}/d\text{PSS})_3/(\text{BCM}/d\text{PSS})_n/(\text{PDMA}/d\text{PSS})_3$, where $n = 1$ and 2. Deposition was performed in 0.2 mg mL^{-1} solutions at pH 6.0 and 45 °C for all polymers. At each step, wafers were immersed in polymer solution for 15 min and then washed in the 0.01 M phosphate buffer for 1 min. The samples were blow-dried with dry nitrogen, kept for 1 week exposed to ambient air, then measured at Oak Ridge National Lab (ORNL).

Ellipsometry

Measurements of dry multilayer thicknesses were performed using a custom-built, single-wavelength, phase-modulated ellipsometer at a 65° angle of incidence. The refractive indices for the native silicon oxide layer and dry multilayer films on a silicon substrate were set at 1.456 and 1.500, respectively. The thickness of each layer was measured after being blown-dry by nitrogen. Measurements of the swelling of multilayer films were performed *in situ* using a custom-made cylindrical flow-through glass cell. The cell was filled with 0.01 M phosphate buffer. Each sample was equilibrated for a minimum of 15 min prior to measurements.

Atomic force microscopy (AFM)

An NSCRIPTOR dip pen nanolithography system (Nanoink) operating in tapping (for dry scans) and contact (for *in situ* scans) modes was used to characterize films.

Neutron reflectometry (NR)

NR measurements were performed using the Spallation Neutron Source Liquids Reflectometer in Oak Ridge National Lab, TN. The reflectivity data were collected in a continuous wavelength band (2.5 Å < λ < 5.75 Å), at a sequence of different incident angles: $\theta = 0.15$, 0.25, 0.45, 0.65, 0.85, 1.60, and 2.80° spanning a momentum transfer ($Q = 4\pi\sin\theta/\lambda$) range of 0.006 Å^{-1} < Q < 0.245 Å^{-1}. The reflectivity curves were assembled by stitching the six different angle datasets together, and a constant instrument resolution was maintained at $\delta Q/Q = 0.05$ for all seven angles by varying the incident-beam apertures. The sample cell for *in situ* NR measurements consisted of a thick silicon disk 2″ in diameter sealed with a rubber O-ring against the sample surface. Inlet and outlet ports on the Si block (1 mm wide drilled holes) were sealed after filling the cell with 5 mL of pH 6.0 0.01 M phosphate buffer solution. The two-Si-block sandwich was clamped onto a ceramic base through an aluminum top plate.

NR data collected for alternating LbL films were analyzed using a model developed for NR studies of hydrogen-bonded multilayers.[21] Since the material in individual PE layers typically extends over several nominal bilayer thicknesses (as determined by the total amount of material deposited) and the scattering densities of the protonated PSS and BCM are similar, we average the protonated-layer scattering densities and model the *d*PSS markers as immersed in this average protonated material. Thicknesses, scattering densities, and interfacial widths were modified iteratively until reflectivity curves were best fitted (minimum χ^2), with interfacial widths, σ_{fwhm}, parameterized as full-width-at-half-maximum, $2.35 \times \sigma_{rms}$. For stacked LbL films, a three-layer model was created, in which SLDs for the top and bottom $(d\text{PSS/PDMA})_3$ layers, and the $(\text{BCM}/d\text{PSS})_n$ layer were averaged.

Results and discussion

To form BCMs, we used the PNIPAM-*b*-PDMA copolymer with a 25 : 50 ratio of repeat units as determined by a combination of GPC and ^{1}H NMR. In aqueous solutions at pH 6.0 and temperatures above PNIPAM's LCST of 32 °C, this copolymer formed micelles with PNIPAM cores (R_h of ~18 nm). The smaller value of R_h of these BCMs compared to R_h ~ 35 nm of similar PNIPAM-*b*-PDMA micelles described in our previous studies[31,35] is explained by a smaller block length of the copolymer used here (25 : 50 *vs.* 97 : 57). Whereas in solution amphiphilic micelles dissociate to unimers under conditions which render micellar cores hydrophilic, and BCM assembly within LbL films prevented micellar dissociation as a result of the binding of BCM coronal chains with their polymer counterparts.[31] To investigate water uptake within films with different architectures, we prepared two types of multilayers,

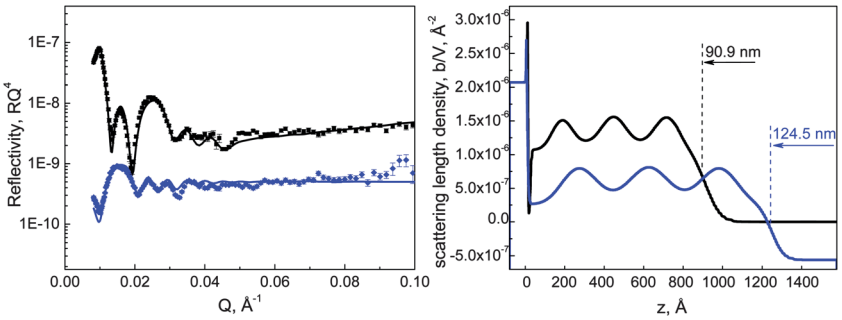

Fig. 1 NR data (left) and SLD profiles (right) of the dry BPEI/PSS/[(BCM/PSS)$_4$/BCM/*d*PSS]$_3$/(BCM/PSS)$_4$ film (black curve) and of the film swollen at 25 °C (blue curve) in 0.01 M phosphate buffer at pH 6.0.

denoted below as alternating and stacked films. For the films of the first type, we assembled a BCM/PSS alternating multilayer film. To study swelling of individual BCM layers we designed a second, stacked system, consisting of three stacks, where a layer of micelles was sandwiched between stacks of linear homopolymers, PSS and PDMA.

Alternating LbL system

Similar to our previously reported data, BPM/PSS multilayer deposition occurred in a linear manner.[31] The first layer of micelles covered ~40% of the surface (a dry ellipsometric thickness of ~2 nm), with a further increase of 5 ± 1 nm per bilayer observed for layers 3 and higher (data not shown). Fig. 1, black curve, shows NR data from a dry 19-bilayer BPM/PSS film deposited at pH 6.0. The data are presented as neutron reflectivity $R \times Q^4$ plotted as a function of momentum transfer Q. The scattering density, layer thickness and internal roughness within the multilayer films shown in Fig. 1 are summarized in Table S1 in the ESI.† The dry thickness of the film was 909 Å, in good agreement with ellipsometry data. A well-defined Bragg peak is seen in the data. In order to fit the data, the thickness of the diffuse *d*PSS marker layers was 110 Å, indicating interpenetration of the *d*PSS chains into neighboring layers. The scattering length density (SLD) of the *d*PSS-containing layers was significantly smaller than the SLD of bulk *d*PSS (1.68×10^{-6} *vs.* 3.80×10^{-6} Å^{-2}) confirming the interdiffusion of macromolecular chains within the film. Hydrogenated polymer layers were fitted as a homogeneous stack with a total thickness of 165 Å. The fact that this value is lower than the dry thickness of a 4.5-bilayer BCM/PSS stack (225 Å measured by ellipsometry) is again consistent with significant interpenetration of *d*PSS within hydrogenated BCM/PSS layers. Note that the thickness of the closest-to-the-substrate four-bilayer BCM/PSS stack was 56 Å smaller than that of the stacks deposited later, because of lower surface coverage within the surface-adsorbed micellar layer.[31] This incomplete substrate coverage by micelles results in a significant surface roughness (22.4 Å, Fig. S2†), as reported in several studies,[26,28,31] which results in a highly diffuse distribution of PSS within the film. Because of persistent interdigitation of micelles, BCM/PSS films are grainy and rough, as shown in the AFM image of a dry 19-bilayer film in Fig. 2A. Values of rms

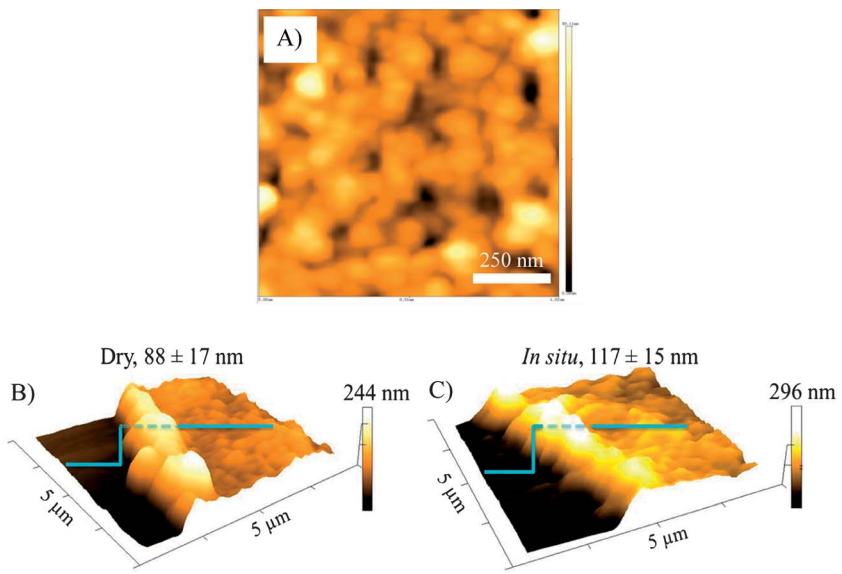

Fig. 2 AFM images of a (BCM/PSS)$_{19}$ dry film (A and B), and a film exposed to 0.01 M phosphate buffer solution at pH 6.0 and 25 °C (C).

roughness measured by AFM [~150 Å for the $(BCM/PSS)_{19}$ film] are comparable to the film internal roughness of 110 Å, indicating a correlation between micellar interdigitation, film disorder and the spatial distribution of PSS chains within the film.

Fig. 1 also shows *in situ* NR data obtained after immersing the 19-bilayer BCM/PSS multilayer film in 0.01 M phosphate buffer at pH 6.0. A set of well-developed Kiessig fringes and a Bragg peak signals the preservation of the layered structure of the film. The fitting procedure was similar to that used for the dry film described above. The total film thickness of 1235 Å indicates a 36% swelling as a result of PE film hydration due to water uptake within BCM's PNIPAM cores. This degree of film swelling is consistent with that determined from the reduction of the SLD values of *d*PSS marker layers from 1.68×10^{-6} to 0.94×10^{-6} Å^{-2} (data are summarized in Table S2†) giving an average water uptake of 36 ± 3%. A larger increase in thickness of *d*PSS marker layers from 110 to 160 Å (~45%) suggests additional spreading of *d*PSS macromolecules into neighboring hydrogenated stacks. In the alternating BCM/PSS films, water uptake was therefore homogeneous because of a high degree of interdigitation between BCM and PSS layers.

Swelling of BCM/PSS multilayers was also studied by *in situ* AFM and ellipsometry. Fig. 2 illustrates the swelling of a $(BCM/PSS)_{19}$ film studied by *in situ* AFM. AFM step analysis showed an 88 ± 17 nm thickness for dry films, and 119 ± 15 nm in *in situ* measurement at 25 °C reflecting a 35% swelling (Fig. 2).

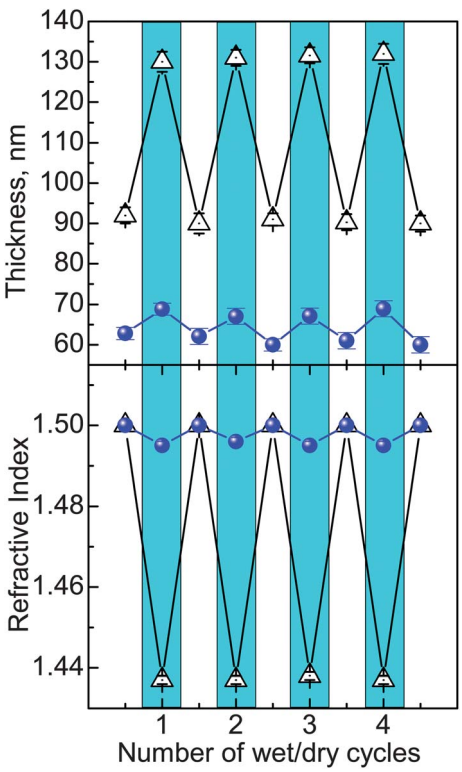

Fig. 3 Ellipsometric thickness (top) and refractive index (bottom) for alternatively deposited $(BCM/PSS)_{19}$ (triangles) and $(PDMS/PSS)_{19}$ (circles) films measured dry (white areas) and *in situ* in 0.01 M phosphate buffer solution at pH 6.0 and 25 °C (blue areas).

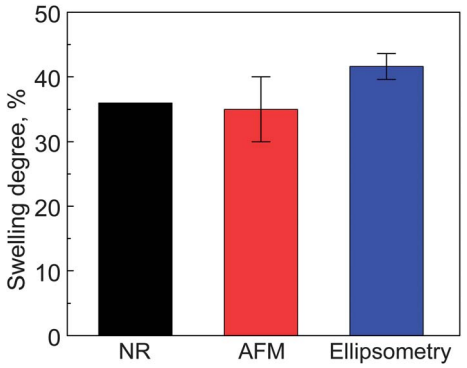

Fig. 4 Swelling degree of $(BCM/PSS)_{19}$ films after their exposure to 0.01 M phosphate buffer solution at pH 6.0 as measured by various techniques.

Importantly, in agreement with earlier studies,[28,31,33] micelles remained intact within the multilayer films as a result of protection with a PSS overlayer. Preservation of micellar morphology before and after *in situ* measurements with BCM-containing films is confirmed by AFM (Fig. S2†). Consistent with AFM data, *in situ* ellipsometry indicated the film reversibly swelled by 41.6% from its dry thickness of 92 ± 2 nm upon exposure to buffer solution at 25 °C. This swelling was accompanied by changes in refractive index from 1.500 to 1.437 for the wet film (Fig. 3). Interestingly, $(PDMA/PSS)_{19}$ multilayers deposited under the same conditions as a control system were significantly thinner (3.2 nm per bilayer) and exhibited only 8 ± 2% reversible swelling upon exposure to 0.01 M phosphate buffer solution at pH 6.0 (Fig. 3, circles).

Fig. 4 shows that different techniques gave consistent values for water uptake within BCM/PSS alternating films. The average swelling degree determined using NR, AFM and an ellipsometry of 38 ± 3%, however, was smaller than swelling for a similar BCM/PSS system of 65% reported in our previous work.[31] This difference can be explained by the 4-fold shorter length of the core-forming PNIPAM block (25 *vs.* 97 monomer units, respectively) in the PNIPAM-*b*-PDMA copolymer in this work as compared to our previous study.

Stacked LbL systems

To extend our study of micelle swelling within multilayer films we designed LbL systems where a layer of micelles was sandwiched between two sequentially deposited three-bilayer stacks of linear homopolymers, PDMA and *d*PSS. We have constructed two types of stacked films (schematically shown in Fig. 5A and 6A), with layer deposition sequences BPEI/*d*PSS/$(PDMA/dPSS)_3$/$(BCM/dPSS)_n$/$(PDMA/dPSS)_3$, where $n = 1$ and 2, differing only in the number of deposited micelle layers. In other words, a micellar BCM/*d*PSS stack was constructed with either one (denoted as single-micellar) or two (denoted as double-micellar) deposition steps. The rationale behind such a choice was to intentionally create partially filled ($n = 1$) and completely filled ($n = 2$) micellar spacer layers within the film. As shown in our previous work, a single adsorption cycle of PNIPAM-*b*-PDMA micelles results in a relatively low limiting surface coverage of micelles (~40%[31]), which is probably explained by increased

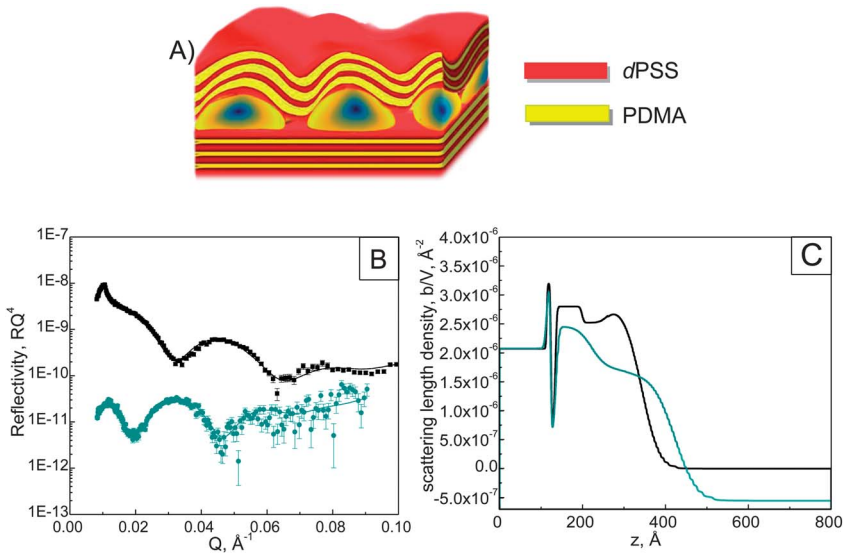

Fig. 5 Schematic representation (A), NR data (B) and SLD profile (C) of dry (black) and swollen (green) BPEI/*d*PSS/(PDMA/*d*PSS)$_3$/(BCM/*d*PSS)$_n$/(PDMA/*d*PSS)$_3$ films with $n = 1$. Swelling of the film was performed in 0.01 M phosphate buffer solution at pH 6.0 and 25 °C.

micellar footprints upon binding of micellar coronas on a precursor-coated silicon wafer. In our experiments, we have observed a similar sparse coverage of micellar monolayers on top of BPEI/*d*PSS/(PDMA/*d*PSS)$_3$ homopolymer stacks (Fig. S1†). Also consistent with incomplete single-deposition micellar coverage is the fact that the dry ellipsometric thickness of the BCM/PSS bilayer of ~3 nm is significantly smaller than the individual height of adsorbed micelles of 6.5 nm as determined by AFM (Fig. S1†).

Fig. 5 and 6 and Tables S3–S6† summarize NR data obtained with multilayers containing BCMs deposited within single and double cycles ($n = 1$ and 2, respectively), and stacked between two homopolymer PDMA/*d*PSS strata. As seen from NR measurements of dry films with a partial micellar layer (Fig. 5, black curve), homopolymer strata and the micellar layer are clearly resolved, with the micellar layer featuring a lower neutron scattering density, as expected from the low value of neutron SLD of PNIPAM-*b*-PDMA micelles of 7.2×10^{-7} Å^{-2} (calculated). However, the observed SLD in the micellar region is much higher (2.52×10^{-6} Å^{-2}), indicating significant intrusion of *d*PSS into intermicellar spaces. The SLD of the bottom PDMA/*d*PSS stack (2.84×10^{-6} Å^{-2}) implies a film composition of 65 : 35 *d*PSS : PDMA. One interesting observation is that the internal roughnesses between the micellar layer and the bottom and top homopolymer stacks were drastically different (9 Å and 35 Å, respectively). This fact further confirms strong intermixing of the top homopolymer stack with the micellar layer. Finally, a lower-SLD micellar layer of thickness 62 Å is clearly observed for the dry film.

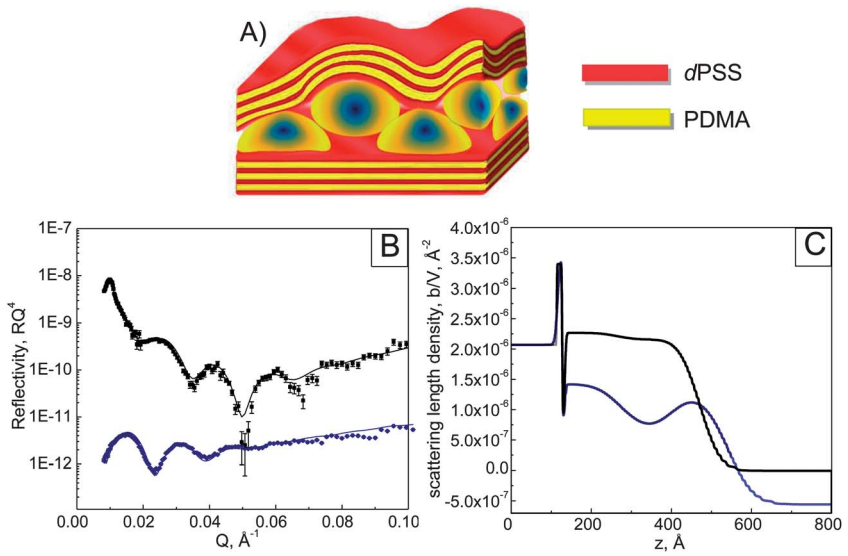

Fig. 6 Schematic representation (A), NR data (B) and SLD profile (C) of dry (black) and swollen (blue) BPEI/*d*PSS/(PDMA/*d*PSS)$_3$/(BCM/*d*PSS)$_n$/(PDMA/*d*PSS)$_3$ systems with $n = 2$. Swelling of the film was performed in 0.01 M phosphate buffer solution at pH 6.0 and 25 °C.

The observed contrasts in the SLD of the film drastically differ after the film is exposed to buffer solution at 25 °C. NR data, taken *in situ* with a single-micellar-layer film, reveal significant differences in the water uptake by the different film stacks. Water uptake by the bottom homopolymer stack was modest (14 ± 5% as estimated from the thickness increase and ~11% as estimated from a decrease in SLD). In contrast, the micellar and top homopolymer stacks became indistinguishable in the wet state and could be successfully fitted by a single layer (Table S4†). This combined top micelle-homopolymer stack demonstrated a swelling degree of 30 ± 5%, as calculated from SLD, and 38 ± 1% as indicated by changes in thickness (an increase from 146 to 202 Å from dry to wet). The fact that the micellar layer and the top homopolymer stack could be fitted as a single stratum reflects "wrapping" of homopolymers around micelles and their penetration into intermicellar spaces during multilayer construction. The higher degree of swelling of this combined stratum as compared to the base homopolymer stratum (~30 to 36% *vs.* 11–14%) is due to strong uptake of water within the core-forming PNIPAM blocks of assembled PNIPAM-*b*-PDMA micelles. Unlike PDMA blocks which participate in binding with *d*PSS, PNIPAM blocks are not involved in intermolecular interactions and are highly swellable by water at temperatures lower than PNIPAM's LCST of 32 °C. The swelling of the homopolymer stack is comparable with earlier studies.[36–38] Values from 20 to ≥40% for water uptake have been reported. However, the high salt concentration of the polymer solutions used in these studies resulted in highly hydrated films due to deposition of the polymer chains in more "fluffy" chain conformations. In our case, films were deposited from 0.01 M salt concentrations and were less hydrated because of thinner, more strongly bound polymer layers.

What, then, of the water uptake in layers with a smaller degree of interpenetration of the homopolymer stack into the micellar layer? This question was addressed with double-micellar films whose schematic structure is shown in Fig. 6A. These films were constructed by applying two deposition cycles of micelles, with a single layer of *d*PSS deposited in-between. Using a fitting procedure similar to the one used above for the single-micellar films, the individual micellar strata were indistinguishable, due to the spreading of *d*PSS into and over the micelles. As seen from the SLD profile, there is almost no difference in SLD over the entire film. After exposure to buffer at 25 °C, the *in situ* NR profile drastically changed, clearly showing the preferential uptake of water into the double-deposition ($n = 2$) micellar layer as compared to the homopolymer base and top stacks. Interestingly, constructing a complete-micellar layer by applying double BCM deposition cycle minimized interdigitation of the top homopolymer stack into the micelles (see scheme in Fig. 6), enabling evaluation of water uptake within individual film stacks. Fig. 6C shows that the double-micellar layer, "sandwiched" between the two homopolymer stacks, showed a significant decrease in SLD for the micelle layer as compared to bottom and top stacks, reflecting ~37% water uptake by the micellar stack, as compared to ~20% by the homopolymer stacks. We suggest that the slightly increased swelling of the film as compared to the film with a partial micellar layer can be explained by the presence of air voids which causes extra water uptake upon swelling. This is also consistent with the fact that the SLD of the dry film is slightly lower than for the film with a partial micellar layer. NR measurements of the dry film after exposure to buffer solution (Fig. S3†) showed a decrease in film thickness from 338 to 285 Å, as well as a 5% increase in SLD, suggesting compaction of the film due to micelle rearrangements, and a partial loss of material after the first swelling cycle. In addition, some intermixing between micellar layers and the bottom homopolymer stack can occur during micelle deposition (suggested by larger σ_{fwhm} values for double-micellar as compared to single-micellar films), leading to higher water uptake by the bottom stack in the first case. Further NR experiments involving variation of buffer solution contrast are required to determine quantitatively the respective contributions of mass loss and voids to the swelling of these films. Importantly, further cycling between dry and swollen states did not result in any changes in either SLD or film thickness. Differences in the swelling stability of films with partial micellar and complete micellar layers allow us to conclude that deposition of homopolymer stack layers results in stronger stabilization of responsive micelles during their swelling response when the micellar layer is incomplete (see Fig. 5A). In this case, the multilayer stack can be 'wrapped around' a larger fraction of the micellar surface, thus preventing the loss of the diblock copolymer material induced by micellar swelling.

Conclusions

In summary, we have studied the internal structure and swelling behavior of BCM-containing films. NR study of alternatively deposited multilayers of BCM with PSS indicated a strongly interdigitated film structure featuring diffuse *d*PSS marker layers. Swelling of such films was homogeneous with a water uptake of 36%, as also confirmed by AFM and ellipsometry. We also showed that controlling film architecture is a powerful tool to create films demonstrating selective swelling within specific film strata. Stacked films showed highly distinct swelling for film homopolymer strata relative to that of the layer of micelles. This distinguishing feature can be used to create materials with controllable selective swelling behavior. By varying the ratio and nature of differently swellable stacks, a broad range of soft materials useful in microfluidics, separations and biomedical technologies can be constructed.

Acknowledgements

This work was supported by the National Science Foundation under Award DMR-0906474.

References

1 G. Decher, Y. Lvov and J. Schmitt, *Thin Solid Films*, 1994, **244**, 772.
2 G. Decher, M. Eckle, J. Schmitt and B. Struth, *Curr. Opin. Colloid Interface Sci.*, 1998, **3**, 3.

3 E. Kharlampieva, J. F. Ankner, M. Rubinstein and S. A. Sukhishvili, *Phys. Rev. Lett.*, 2008, **100**, 128303.
4 E. Kharlampieva, V. Kozlovskaya and S. A. Sukhishvili, *Adv. Mater.*, 2009, **21**, 3053.
5 L. Xu, D. Pristinski, A. Zhuk, C. Stoddart, J. F. Ankner and S. A. Sukhishvili, *Macromolecules*, 2012, **45**, 389.
6 S. S. Shiratori and M. F. Rubner, *Macromolecules*, 2000, **33**, 4213.
7 M. Müller, T. Rieser, K. Lunkwitz, S. Berwald, J. Meier-Haack and D. Jehnichen, *Macromol. Rapid Commun.*, 1998, **19**, 333.
8 D. Yoo, S. S. Shiratori and M. F. Rubner, *Macromolecules*, 1998, **31**, 4309.
9 K. Glinel, A. Moussa, A. M. Jonas and A. Laschevsky, *Langmuir*, 2002, **18**, 1408.
10 J. H. Jeremy and M. L. Bruening, *Langmuir*, 2000, **16**, 2006.
11 E. Kharlampieva, V. Kozlovskaya, J. Chan, J. F. Ankner and V. V. Tsukruk, *Langmuir*, 2009, **25**, 14017.
12 S. T. Dubas and J. B. Schlenoff, *Macromolecules*, 1999, **32**, 8153.
13 J. D. Mendelsohn, C. J. Barrett, V. V. Chan, A. J. Pal, A. M. Mayes and M. F. Rubner, *Langmuir*, 2000, **16**, 5017.
14 G. Decher and L. Schmitt, *Prog. Colloid Polym. Sci.*, 1992, **89**, 160.
15 G. Decher, in *Comprehensive Supramolecular Chemistry*, ed. J. P. Sauvage and M. W. Hosseini, Pergamon Press, Oxford, 1996, vol. 9, ch. 14.
16 G. Decher, *Science*, 1997, **277**, 1232.
17 J. Schmitt, T. Grünewald, G. Decher, P. S. Pershan, K. Kjaer and M. Lösche, *Macromolecules*, 1993, **26**, 7058.
18 R. Kügler, J. Schmitt and W. Knoll, *Macromol. Chem. Phys.*, 2002, **203**, 413.
19 M. Lösche, J. Schmitt, G. Decher, W. G. Bouwman and K. Kjaer, *Macromolecules*, 1998, **31**, 8893.
20 G. J. Kellogg, A. M. Mayes, W. B. Stockton, M. Ferreira and M. F. Rubner, *Langmuir*, 1996, **12**, 5109.
21 E. Kharlampieva, V. Kozlovskaya, J. F. Ankner and S. A. Sukhishvili, *Langmuir*, 2008, **24**, 11346.
22 G. B. Webber, E. J. Wanless, S. P. Armes, Y. Tang, Y. Li and S. Biggs, *Adv. Mater.*, 2004, **16**, 1794.
23 K. Emoto, M. Iijima, Y. Nagasaki and K. Kataoka, *J. Am. Chem. Soc.*, 2000, **122**, 2653.
24 N. Ma, H. Zhang, B. Song, Z. Wang and X. Zhang, *Chem. Mater.*, 2005, **17**, 5065.
25 P. M. Nguyen, N. S. Zacharia, E. Verploegen and P. T. Hammond, *Chem. Mater.*, 2007, **19**, 5524.
26 I. Erel, Z. Zhu, A. Zhuk and S. A. Sukhishvili, *J. Colloid Interface Sci.*, 2011, **355**, 61.
27 I. Erel, H. E. Karahan, C. Tuncer, V. Bütün and A. L. Demirel, *Soft Matter*, 2012, **8**, 827.
28 Z. Zhu and S. A. Sukhishvili, *ACS Nano*, 2009, **3**, 3595.
29 J. Cho, J. Hong, K. Char and F. Caruso, *J. Am. Chem. Soc.*, 2006, **128**, 9935.
30 J. Hong, W. K. Bae, H. Lee, S. Oh, K. Char, F. Caruso and J. Cho, *Adv. Mater.*, 2007, **19**, 4364.
31 L. Xu, Z. Zhu and S. A. Sukhishvili, *Langmuir*, 2011, **27**, 409.
32 W. S. Tan, R. E. Cohen, M. F. Rubner and S. A. Sukhishvili, *Macromolecules*, 2010, **43**, 1950.
33 W. S. Tan, Z. Zhu, S. A. Sukhishvili, M. F. Rubner and R. E. Cohen, *Macromolecules*, 2011, **44**, 7767.
34 I. Ydens, S. Moins, P. Degeé and P. Dubois, *Eur. Polym. J.*, 2005, **41**, 1502.
35 L. Xu, Z. Zhu, O. V. Borisov, E. B. Zhulina and S. A. Sukhishvili, *Phys. Rev. Lett.*, 2009, **103**, 118301.
36 M. Lösche, J. Schmitt, G. Decher, W. G. Bouwman and K. Kjaer, *Macromolecules*, 1998, **31**, 8893.
37 J. Wong, F. Rehfeldt, P. Hänni, M. Takana and R. Klitzing, *Macromolecules*, 2004, **37**, 7285.
38 R. Köhler, I. Dönch, P. Ott, A. Laschewsky, A. Fery and R. Krastev, *Langmuir*, 2009, **25**, 11576.